

## Nanopore and Nanobushing Arrays from ABC Triblock Thin Films Containing Two Etchable Blocks

Shouwu Guo, Javid Rzayev, Travis S. Bailey, Andrew S. Zalusky, Roberto Olayo-Valles, and Marc A. Hillmyer\*

Department of Chemistry, University of Minnesota, 207 Pleasant Street SE, Minneapolis, Minnesota 55455-0431

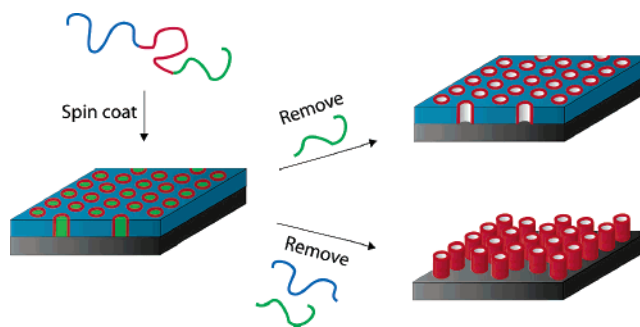
Received December 6, 2005

Revised Manuscript Received February 15, 2006

In 1997, Park et al. reported that thin films of simple polystyrene (PS)–polydiene block copolymers could be manipulated by a combination of chemical degradation and reactive ion etch (RIE) processes to generate nanoporous thin film stencils useful for fabrication of large area arrays of nanodots or nanopits on a SiN substrate.<sup>1</sup> This report spurred a flurry of activity in the area of block copolymer nanolithography, a technique that enables the patterning of large areas by simple spin coating of the block copolymer as a thin film combined with thermal, chemical, and/or irradiation steps.<sup>2</sup> The use of block copolymers as templates or template precursors is extremely attractive for several reasons: block copolymers inherently phase separate on a nanometer length scale,<sup>3</sup> various techniques are available for their synthesis,<sup>4</sup> and the understanding of diblock copolymer thin film self-assembly is well-established.<sup>5</sup> The preparation of advanced structures such as nanoscopic metal-oxide-semiconductor capacitors as well as large area, metallic<sup>6</sup> and magnetic<sup>7</sup> nanodot arrays has been demonstrated.<sup>8</sup> This area has been recently reviewed, and the reader is referred to references 9 and 10 for comprehensive examinations of this field.

While the demonstrated and potential utility of AB diblock copolymers in nanolithography is remarkable, there are only a limited number of structures adopted by diblock copolymer thin films.<sup>5</sup> This renders AB diblock copolymers only generally useful for the production of nanoscopic lines, trenches, dots, and pits. Given this limitation, we reasoned that the diversity of structures observed in ABC triblock terpolymers<sup>11</sup> would facilitate the fabrication of films useful for templating structures with more complex two-dimensional

### Scheme 1. Schematic Representation of the Envisioned Nanotemplates from Thin Films of ABC Triblock Terpolymers



structures such as nanoscopic rings<sup>12</sup> or “antirings”,<sup>13</sup> structures that have generated considerable interest in nanomagnetism.<sup>14</sup> There have been several reports documenting the self-assembly of ABC block terpolymer thin films; various morphologies have been adopted depending on film thickness and solvent annealing conditions.<sup>15</sup> We envisioned that the formation of a core–shell cylindrical morphology in a thin film with the cylinders oriented normal to the substrate could be used as a nanoring template provided either the shell component (Scheme 1, top) or both the core and the matrix components (Scheme 1, bottom) could be selectively removed in a process related to that reported for AB diblock copolymers by Thurn-Albrecht et al.<sup>16</sup> This first requires the synthesis of triblocks containing three chemically distinct components, at least one of which can be selectively etched. Second, the ABC triblocks should form the targeted core–shell cylindrical morphology. Third, thin films of the material must adopt the desired perpendicular orientation.<sup>17</sup> Finally, removal of either the shell component (or both the core and the matrix components) must result in a stable nanostructured thin film. In this communication, we report the formation of the targeted nanostructure arrays shown in Scheme 1 from ABC triblocks containing polystyrene (PS) and two chemically etchable blocks, polyisoprene (PI) and polylactide (PLA).

We prepared a PS–PI–PLA triblock copolymer by sequential anionic polymerization (PS–PI), end capping with

\* To whom correspondence should be addressed. E-mail: hillmyer@chem.umn.edu.

- (1) Park, M.; Harrison, C.; Chaikin, P. M.; Register, R. A.; Adamson, D. H. *Science* **1997**, *276*, 1401.
- (2) Hillmyer, M. A. *Adv. Polym. Sci.* **2005**, *190*.
- (3) Hamley, I. W. *The Physics of Block Copolymers*; Oxford University Press: Oxford, 1998.
- (4) Hillmyer, M. A. *Curr. Opin. Solid State Mater. Sci.* **1999**, *4*, 559.
- (5) Fasalola, M. J.; Mayes, A. M. *Annu. Rev. Mater. Res.* **2001**, *31*, 323.
- (6) For example, see: Shin, K.; Leach, K. A.; Goldbach, J. T.; Kim, D. H.; Jho, J. Y.; Tuominen, M.; Hawker, C. J.; Russell, T. P. *Nano Lett.* **2002**, *2*, 933.
- (7) For example, see: Naito, K.; Hieda, H.; Sakurai, M.; Kamata, Y.; Asakawa, K. *IEEE Trans. Magn.* **2002**, *38*, 1949.
- (8) Black, C. T.; Guarini, K. W.; Milkove, K. R.; Baker, S. M.; Russell, T. P.; Tuominen, M. T. *Appl. Phys. Lett.* **2001**, *79*, 409.
- (9) Li, M.; Coenjarts, C.; Ober, C. K. *Adv. Polym. Sci.* **2005**, *190*, 183.
- (10) Park, C.; Yoon, J.; Thomas, E. L. *Polymer* **2003**, *44*, 6725.
- (11) Abetz, V. *Adv. Polym. Sci.* **2005**, *189*, 125.

- (12) Pearson, D. H.; Tonucci, R. J.; Bussmann, K. M.; Bolde, E. A. *Adv. Mater.* **1999**, *11*, 769.
- (13) Anti-ring array templates would consist of either ring-shaped trenches in a matrix of another material or ring-shaped protrusions on an otherwise flat surface.
- (14) Podbielski, J.; Giesen, E.; Berginski, M.; Hoyer, N.; Grudler, D. *Superlattices Microstruct.* **2005**, *37*, 341.
- (15) For recent relevant work, see the series of S. Ludwigs et al.: (a) Ludwigs, S.; Böker, A.; Voronov, A.; Rehse, N.; Magerle, R.; Krausch, G. *Nat. Mater.* **2003**, *2*, 744. (b) Ludwigs, S.; Schmidt, K.; Stafford, C. M.; Amis, E. J.; Fasalola, M. J.; Karim, A.; Magerle, R.; Krausch, G. *Macromolecules* **2005**, *38*, 1850. (c) Ludwigs, S.; Schmidt, K.; Krausch, G. *Macromolecules* **2005**, *38*, 2376.
- (16) Thurn-Albrecht, T.; Schotter, J.; Kästle, G. A.; Emley, N.; Shibauchi, T.; Krusin-Elbaum, L.; Guarini, K.; Black, C. T.; Tuominen, M. T.; Russell, T. P. *Science* **2000**, *290*, 2126.
- (17) Perpendicular core–shell cylinders have been observed over a limited region of film thicknesses in solvent annealed thin films of PS–poly(vinylpyridine)–poly(*tert*-butyl methacrylate) triblock terpolymers as described in ref 15b.

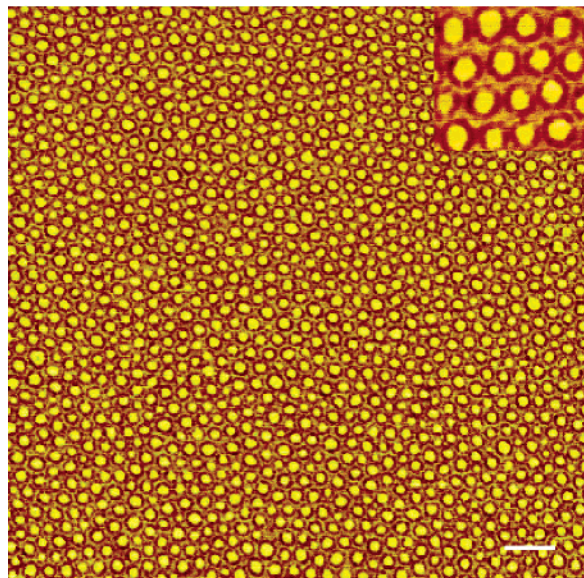


**Figure 1.** Tapping mode AFM phase image acquired from a PS-PI-PLA thin film on a HMDS modified Si substrate after annealing at 150 °C for 15 h under reduced pressure. The scale bar in the lower right is 200 nm. The inset in the upper right is 250 × 250 nm.

ethylene oxide (PS-PI-OH), and subsequent aluminum catalyzed polymerization of lactide (PS-PI-PLA) combining established procedures for the synthesis of PS-PLA<sup>18,19</sup> and PI-PLA<sup>20</sup> diblock copolymers and using a protocol related to that published by Bailey et al. for the synthesis of PS-PI-PEO ABC triblocks.<sup>21</sup> PS-PI-PLA had an overall number-averaged molecular weight ( $M_n$ ) of 65 kg mol<sup>-1</sup>, a polydispersity index (PDI) of 1.09, and the following weight fractions: PS 60%, PI 11%, and PLA 29%. By small-angle X-ray scattering (SAXS) analysis, bulk samples of this material formed a microphase separated structure, evidenced by the appearance of a principal scattering peak (Figure S1, Supporting Information). However, weak and broad higher order reflections prohibited definitive identification of the morphology. Remarkably, a thin (ca. 65 nm) film of PS-PI-PLA spin cast on Si with a native oxide layer (ca. 100 nm thick) hydrophobically modified by hexamethyldisilazane (HMDS), annealed at 150 °C for 15 h and analyzed by atomic force microscopy (AFM) in the tapping mode, gave the image shown in Figure 1. Thicker films (100 and 170 nm) also provided similar AFM images. Given the three distinct levels of contrast, hexagonally packed regions of a core-shell cylindrical morphology are apparent from this image. The mean center-to-center distance of these features (as determined by fast Fourier transform (FFT) analysis on AFM images) is 65 nm and compares favorably to the SAXS data (63 nm) assuming hexagonally packed core-shell cylinders (Figure S1, Supporting Information). Larger area AFM images (4 × 4 μm<sup>2</sup>) and several areas of the same film showed a morphology similar to that in Figure 1. The dark ring surrounding the light circular features suggests that

the softest and/or most hydrophobic material constitutes the shells.<sup>22</sup> Thus, we conclude that the hydrophobic, low glass transition PI surrounds the stiff, least hydrophobic PLA component and that PS constitutes the continuous matrix phase (consistent with the connectivity and relative lengths of the blocks in the terpolymer). Selective removal of the PI would generate the desired nanoring templates (Scheme 1) with inner and outer diameters of approximately 37 and 63 nm, respectively.

We attempted to remove the PI component from the thin films shown in Figure 1 by ozonolysis (treatment with O<sub>3</sub> as in reference 23). However, our attempts to selectively remove the PI led to concomitant partial removal of the PLA component (as determined by NMR analysis post O<sub>3</sub> treatment), and the nanoporous structures generated were reminiscent of those generated from simple PS-PLA diblock copolymers.<sup>24</sup> In fact, the PLA component could be selectively removed (by treatment with NaOH solutions) from the PS-PI-PLA triblocks to generate nanoporous templates useful for the fabrication of either pits in SiO<sub>2</sub> by consecutive O<sub>2</sub> and CF<sub>4</sub> RIE steps or gold nanodot arrays by a combination of O<sub>2</sub> RIE, gold deposition, and mask lift off as established for PS-PLA diblock copolymer templates (Figure S2, Supporting Information).<sup>24</sup> The necessity of an O<sub>2</sub> RIE step in both pattern transfer processes suggests that the surface morphology depicted in Figure 1 does not span the entire film thickness; instead, a layer of material (presumably PS) coats the hydrophobically modified SiO<sub>2</sub> surface as seen in previous work with PS-PLA thin films on this substrate.<sup>25</sup> Nonetheless, we showed that simple PLA degradation and RIE processing enabled the use of these ABC materials as nanolithographic templates. In addition, nanoporous films obtained after PLA removal contain a reactive PI layer on the interior pore surface, providing opportunities to further manipulate the local pore environment.<sup>26</sup>

The partial success of our approach with PS-PI-PLA materials suggested that related PI-PS-PLA materials could lead to core-shell cylindrical materials with a robust PS shell provided the appropriate composition was obtained. Degradation of both the PI and the PLA would lead to the “anti-ring” templates shown in Scheme 1. To that end, using a similar synthetic procedure we prepared a PI-PS-PLA triblock with an overall  $M_n$  of 18 kg mol<sup>-1</sup>, a PDI of 1.11, and the following weight fractions PI 32%, PS 38%, and PLA 30%. SAXS analysis of this material at 160 °C suggests hexagonal symmetry (Figure S3, Supporting Information), and thin films of PI-PS-PLA (ca. 60 nm on HMDS modified SiO<sub>2</sub>) exhibited patches of hexagonally packed features over large areas upon annealing under reduced pressure at 120 °C for 12 h (Figure 2).<sup>24,27</sup> Films up to 210 nm thick showed similar AFM images but required higher

(18) Zalusky, A. S.; Olayo-Valles, R.; Taylor, C. J.; Hillmyer, M. A. *J. Am. Chem. Soc.* **2001**, *123*, 1519.

(19) Zalusky, A. S.; Olayo-Valles, R.; Wolf, J. H.; Hillmyer, M. A. *J. Am. Chem. Soc.* **2002**, *124*, 12761.

(20) Schmidt, S. C.; Hillmyer, M. A. *Macromolecules* **1999**, *32*, 4794.

(21) Bailey, T. S.; Pham, H. D.; Bates, F. S. *Macromolecules* **2001**, *34*, 6994.

(22) Whangbo, M. H.; Cleveland, J.; Elings, V.; Denley, D.; Magonov, S. N. *Surf. Sci.* **1997**, *389*, 201.

(23) Collins, S.; Hamley, I. W.; Mykhaylyk, T. *Polymer* **2003**, *44*, 2403.

(24) Olayo-Valles, R.; Lund, M. S.; Leighton, C.; Hillmyer, M. A. *J. Mater. Chem.* **2004**, *14*, 2729.

(25) Olayo-Valles, R.; Guo, S.; Lund, M. S.; Leighton, C.; Hillmyer, M. A. *Macromolecules* **2005**, *38*, 10101.

(26) For related work, see: (a) Rzaev, J.; Hillmyer, M. A. *Macromolecules* **2005**, *38*, 3. (b) Rzaev, J.; Hillmyer, M. A. *J. Am. Chem. Soc.* **2005**, *127*, 13373.

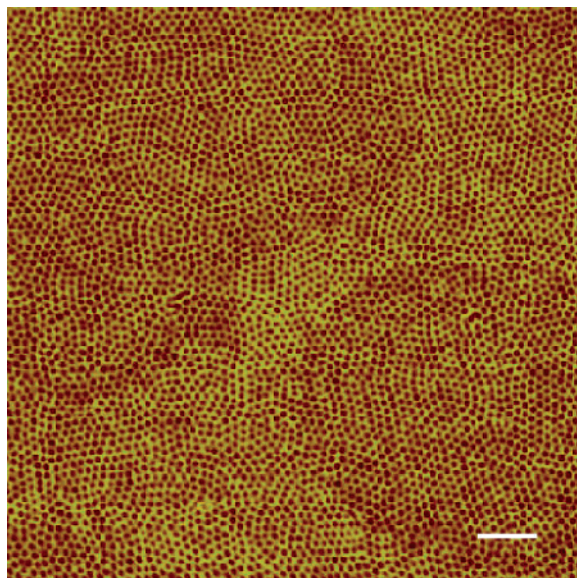


**Figure 2.** Tapping mode AFM phase image of a PI-PS-PLA thin film on a HMDS modified Si substrate after annealing at 120 °C for 12 h under reduced pressure. The scale bar in the lower right is 200 nm.

annealing temperatures (180 °C). Larger area AFM images ( $4 \times 4 \mu\text{m}^2$ ) and several areas of the same film showed a morphology similar to that in Figure 2. Unlike the AFM image shown in Figure 1, only two levels of contrast were observed in Figure 2, and, therefore, definitive assignment of the morphology was more difficult, although the putative cylindrical domains were likely softer and more hydrophobic than the continuous matrix phase, given the observed AFM contrast.<sup>22</sup> By staining the sample with  $\text{OsO}_4$  (selective for PI) and imaging the sample by Scanning electron microscopy (SEM; Figure S4, Supporting Information), we were able to demonstrate that the interior of the cylindrical domains was composed of PI. Bright circular features in the SEM image (consistent with high electron density associated with the osmium stain) were smaller in diameter (ca. 15 nm) than those observed in Figure 2 (ca. 25 nm). In further support of cylindrical PI cores, an  $\text{O}_3$  etch of a PI-PS-PLA thin film resulted in nanoscopic pits (Figure S5, Supporting Information) that exhibited the same diameter and spacing as the PI features identified by SEM (Figure S4, Supporting Information). Unlike the PS-PI-PLA films, the  $\text{O}_3$  treatment did not significantly remove the PLA phase (as determined by NMR analysis). This may be due in part to the physical separation of these two components in PI-PS-PLA. Given these data, the connectivity of the blocks, and the component molecular weights, we concluded that the spin cast and annealed PI-PS-PLA thin films form core(PI)-

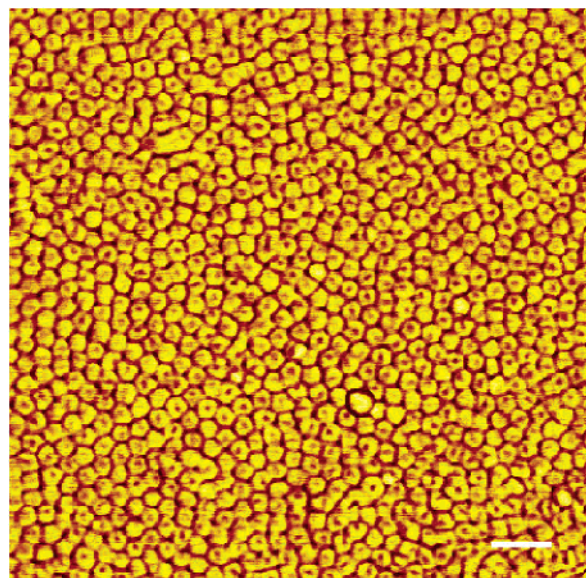


**Figure 3.** Tapping mode AFM phase image of a PI-PS-PLA thin film after sequential treatment with  $\text{O}_3$  and a 0.05 M NaOH solution ( $\text{H}_2\text{O}/\text{MeOH}$ , 23 °C for 45 min). The scale bar in the lower right is 100 nm.

shell(PS) cylinders in a PLA matrix with the cylinder axis oriented normal to the modified  $\text{SiO}_2$  substrate. Although we are not entirely certain that these features span the whole film (i.e., from the free surface to the substrate), repeated  $\text{O}_2$  RIE and AFM imaging suggests this is the case.

Sequential treatment of PI-PS-PLA thin films with  $\text{O}_3$  (2 min,  $-72$  °C, in methanol) and then a 0.05 M NaOH solution (water/methanol at 23 °C for 45 min) led to near complete removal of both the PI and PLA phases, respectively, as determined by  $^1\text{H}$  NMR spectroscopy. An AFM height image suggested the formation of nanoscopic PS pillars similar to those generated by Shin et al.;<sup>6</sup> however, a small hole was observed in the centers of nearly all of the posts (Figure S6, Supporting Information). These features were more prevalent and distinct in the corresponding AFM phase image shown in Figure 3, and we conclude that nanoscopic, hollow, cylindrical PS posts (nanobushings) were generated by this degradation procedure (see Scheme 1).<sup>28</sup> Therefore, in principle, these nanoporous thin films should be effective templates for the generation of metal anti-ring arrays upon deposition and template lift-off; we are currently exploring this possibility. To our knowledge, this is the first example of a nanoporous thin film template with discrete two-dimensional objects.

**Acknowledgment.** This work was supported by the National Science Foundation (DMR-0094144), by the David and Lucile Packard Foundation, and in part by the MRSEC Program of the National Science Foundation under Award No. DMR-0212302.

**Supporting Information Available:** Experimental details and Figures S1–S6 (PDF). This material is available free of charge via the Internet at <http://pubs.acs.org>.

CM052694M

(27) An average center-to-center distance of the features in Figure 2 (as determined by two-dimensional FFT) of 31 nm was in excellent agreement with the value by SAXS analysis of 30 nm.

(28) The holes generated by the removal of the PI core in Figure 3 appear smaller than the holes shown in Figure S5 (Supporting Information). In Figure 3, the PLA has been removed whereas in Figure S5 (Supporting Information) the PLA has not been (significantly) removed. Removal of the PLA phase may have enabled some reconstruction of the PS phase, but at this stage we cannot be certain.